CrystEngComm

ROYAL SOCIETY OF CHEMISTRY

PAPER

View Article Online
View Journal | View Issue

Cite this: *CrystEngComm*, 2025, **27**, 3279

The behaviour of two diamino-derived host compounds in cyclohexanone and isomeric methylcyclohexanones†

Danica B. Trollip, *[a] Benita Barton, [a] Mino R. Caira [b] and Eric C. Hosten [a]

The present investigation centred around the host ability of two novel compounds, *N*,*N*′-bis(5-phenyl-5-dibenzo[*a*,*d*]cycloheptenyl)propane-1,3-diamine (**DB3**) and *N*,*N*′-bis(9-phenyl-9-thioxanthenyl)butane-1,4-diamine (**S4**), for guest solvents cyclohexanone and its methylcyclohexanone isomers (Cyc, 2MeCyc, 3MeCyc and 4MeCyc). While **DB3** formed complexes with each of these organic solvents, **S4** only included 4MeCyc. All complexes were characterized by 1 : 1 host : guest ratios. With the view to assessing whether these host compounds have the potential to separate mixtures of the cyclohexanones, each one was crystallized from various guest mixtures. It was determined that such separations would not be feasible through supramolecular chemistry strategies with these two host species owing to low calculated selectivity coefficients (*K*). This was despite the observed selectivity of **DB3** for 4MeCYC and Cyc in the mixed guest experiments. However, a thorough scrutiny of the five novel complexes was subsequently undertaken, and the crystal structures, through SCXRD analysis, demonstrated that Cyc, a preferred guest solvent, when included by **DB3**, occupied highly constricted channels, while these were comparatively wider and more open in the complexes with the MeCycs. Furthermore, preferred Cyc was the only guest molecule that engaged in a classical hydrogen bond with **DB3**, and Hirshfeld surface analyses showed this guest (which only has 10 hydrogen atoms) to be involved in the greater quantity of (guest)H···H(host) interactions (the MeCyc molecules have 12 hydrogen atoms and experienced less of this type of interaction). All of these observations provide an explanation for the affinity of **DB3** for Cyc (but not for 4MeCyc). These SCXRD analyses further demonstrated that the geometry of the diamino linker in the **DB3** complexes was more folded in nature while, in **S4**·4MeCyc, this was in an extended zig-zag orientation. Finally, thermal analyses on each of the complexes, unsurprisingly, demonstrated the Cyc-containing complex with **DB3** to be the most stable one.

Received 17th March 2025,
Accepted 24th April 2025

DOI: 10.1039/d5ce00298b

rsc.li/crystengcomm

1. Introduction

Cyclohexanone (Cyc) and its methylated isomers (2MeCyc, 3MeCyc and 4MeCyc), when present as mixtures, are extremely difficult to separate using fractional distillations and/or crystallizations as a result of their similar physical properties. To illustrate, Cyc boils at 154.3 °C, while the boiling points of 2MeCyc, 3MeCyc and 4MeCyc are 162–163, 169–170 and 169–171 °C, respectively.[1–4] As a result, these more usual separatory methods become extremely costly with respect to both the energy required as well as the economics involved and, moreover, often render a final product with lower than acceptable purity.[5–7]

These cyclic ketones are prepared by either the catalytic hydrogenation of phenol (in the case of Cyc) and the applicable *o*-, *m*- or *p*-cresol (for the MeCyc isomers),[8] or by dehydrogenation (oxidation) protocols on cyclohexanol and methylcyclohexanol substrates.[9] In the former instance, the cresol employed is frequently not pure but tainted with the other cresol isomers, also as a result of near-identical physical properties, thus resulting in such MeCyc mixtures. Therefore, alternative separation and/or purification strategies that are less energy intensive and more efficient remain attractive.

[a] *Department of Chemistry, Nelson Mandela University, PO Box 77000, Gqeberha (Port Elizabeth), 6031, South Africa. E-mail: s217468225@mandela.ac.za*
[b] *Department of Chemistry, University of Cape Town, Rondebosch 7701, South Africa*

† Electronic supplementary information (ESI) available: The crystal structures of complexes **DB3**·Cyc, **DB3**·2MeCyc, **DB3**·3MeCyc, **DB3**·4MeCyc and **S4**·4MeCyc were deposited at the Cambridge Crystallographic Data Centre (CCDC) and their CCDC numbers are 2349323, 2338003–2338005 and 2429121. Relevant ^{1}H-NMR spectra are provided in Fig. S1 and S2. Table S1 summarises the *K* values calculated for the selectivity profiles. Fig. S3–S11 contain the GC traces for the equimolar experiments and non-equimolar binary experiments. For ESI and crystallographic data in CIF or other electronic format see DOI: **https://doi.org/10.1039/d5ce00298b**

Host–guest chemistry, a branch of the broader supramolecular chemistry field, may serve as a different separation approach for mixtures of isomers and related compounds that have similar physical properties.[10–12] As examples, Bawa and coworkers demonstrated that the host compound 9,10-[2-(9-hydroxy-9-fluorenyl)ethynyl] anthracene possessed an enhanced selectivity for 4-picoline in pyridine/picoline mixtures,[13] while the roof-shaped compound *trans*-α,α,α′,α′-tetra(*p*-chlorophenyl)-9,10-dihydro-9,10-ethanoanthracene-11,12-dimethanol was able to separate binary mixtures of the dichlorobenzene isomers.[14] It has also been reported that Cyc and cyclohexanol mixtures (bp 154.3 and 161.8 °C) may be facilely separated by means of a new RhombicArene:[15] this macrocyclic host compound demonstrated a near-complete selectivity towards the ketone in an adsorptive process that was shown to be rapid and recyclable. Hydrogen bonding and C–H···π interactions were observed in these complexes. Furthermore, host compound (+)-(2*R*,3*R*)-1,1,4,4-tetraphenylbutane-1,2,3,4-tetraol (TETROL) has been presented with mixtures containing Cyc/MeCycs,[16] and unsubstituted Cyc was always the preferred guest solvent in these conditions, followed by 2MeCyc, while when, on the other hand, employing *N*,*N*′-bis(9-phenyl-9-thioxanthenyl)ethylenediamine as the host species, Cyc as well as 2MeCyc were preferentially selected over the remaining two guest solvents.[17]

Host–guest chemistry and complexation processes rely on weak, reversible and non-covalent forces between the host and guest molecules, and these may include hydrogen bonding, C–H···π, π···π stacking and other short contacts.[18–20] The selectivity behaviour of the host species in guest mixtures may be affected by the distance and direction of these interactions as well as the geometry of the guest molecule which may have consequences on the tightness of the packing in the host–guest complex.

In designing effective host compounds, various crystal engineering considerations are requisite. Host compounds should be devised in such a manner that host–guest interactions are promoted since these would facilitate guest retention in the complex. As such, moieties within the host molecule that have hydrogen bonding ability are an advantage if the guest species is also capable of such interactions. Furthermore, host molecules with bulky groups, such as aromatic rings, may provide a surrounding factor for the guest molecules in the complex, and are thus also attractive in the design process, not to mention the plausibility of their becoming involved in π···π stacking and other close contacts involving centres of gravity.

In the present investigation, two novel compounds, *N*,*N*′-bis(5-phenyl-5-dibenzo[*a*,*d*]cycloheptenyl)propane-1,3-diamine (**DB3**) and *N*,*N*′-bis(9-phenyl-9-thioxanthenyl)butane-1,4-diamine (**S4**), were designed as potential host compounds which possessed both these bulky (aromatic) moieties and hydrogen bonding capability (NH functional groups). The synthesis of these compounds was, subsequently, successful, and so they were assessed for their host ability for Cyc and the MeCyc isomers (Scheme 1). The host separatory ability for these cyclic ketones was also investigated through guest competition experiments. Moreover, the five novel compounds produced here were analysed by means of single crystal X-ray diffraction and thermal experiments in order to investigate the non-covalent interactions present and also to assess their relative thermal stabilities. Herein we report on the results so obtained.

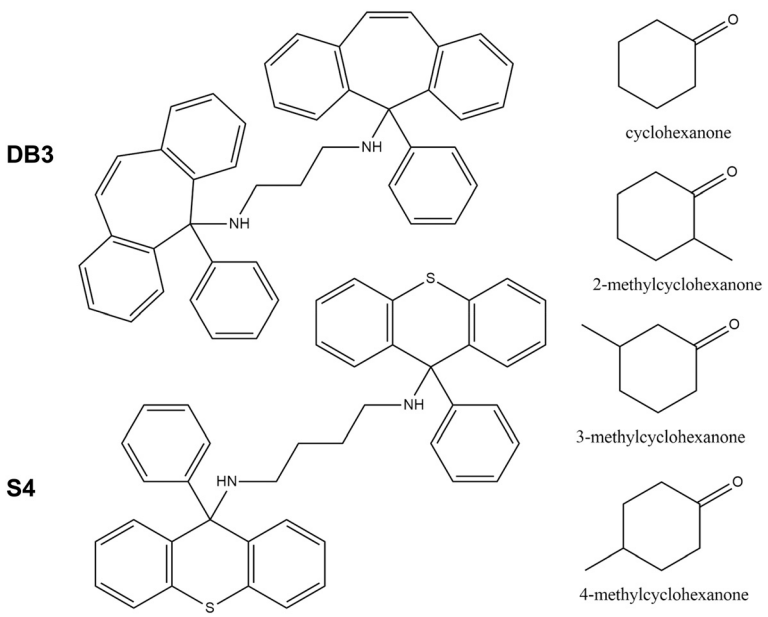

Scheme 1 Structures of the **DB3** and **S4** molecules as well as the potential cyclic ketone guest solvents.

2. Methods

2.1 General

All solvents and chemicals were obtained from Merck (South Africa) and were used without further modification.

A Bruker Ultrashield Plus 400 MHz spectrometer was used for all ^{1}H- and ^{13}C-NMR experiments. $CDCl_3$ was the deuterated solvent, while Topspin 4.2 software was employed for data analysis.

Infrared experiments were carried out using a Bruker Tensor 27 FT-IR spectrometer; OPUS software was the applicable program for spectral analysis.

Melting points were obtained by means of a SMP10 melting point apparatus and are uncorrected.

2.2 Gas chromatography

GC analyses were carried out using a Young Lin YL6500 GC-FID equipped with a Cyclosil-B column. The method involved an initial hold time of 1 min at 60 °C after which the sample was heated to 120 °C with a ramp rate of 10 °C min^{-1} with an additional 1 min hold time at this temperature. Finally, a heating rate of 5 °C min^{-1} was applied until a final temperature of 120 °C was attained. The flow rate was 1.5 mL min^{-1} and the split ratio 1 : 50.

2.3 SCXRD experiments

Two diffractometers were used for the SCXRD experiments. The crystal structure of **S4**·4MeCyc was obtained by means of a Bruker Kappa APEXII diffractometer with graphite-monochromated MoKα radiation (λ = 0.71073 Å). APEXII was used for data-collection while unit cell refinement and data reduction were carried out by means of SAINT.[21] To solve the structures, SHELXT-2018/2 (ref. 22) was employed, whilst refinement required least-squares procedures using SHELXL-2018/3 (ref. 23) together with SHELXLE[24] as a graphical user interface. Carbon-bound hydrogen atoms were added in idealized geometrical positions in a riding model, whilst all non-hydrogen atoms were refined anisotropically. Finally, data were corrected for absorption effects using the numerical method implemented in SADABS.[23] An alternative diffractometer was used for the Cyc-, 2MeCyc-, 3MeCyc- and 4MeCyc-containing complexes of **DB3**. Intensity data were collected on a Bruker D8 VENTURE single crystal X-ray diffractometer using graphite-monochromated MoKα radiation, with the crystal specimen cooled to 100(2) K with nitrogen vapour from a cryostream (Oxford Cryosystems). Data-collection, performed with ω- and ϕ-scans of width 1.0°, was controlled using APEX3/v2019.1-0 (Bruker) software and refinement of the unit cell and data reduction were performed with program SAINT v8.40A (Bruker).[25] Absorption corrections were applied using the multi-scan method with program SADABS (2016/2).[26] The structures were solved by direct methods and refined by full-matrix least-squares (programs in the SHELX suite).[27] As a graphical user interface, version 4.0 of X-Seed (a Program for Supramolecular Crystallography) was employed.[28] In the final cycles of refinement, all non-hydrogen atoms were treated anisotropically, while H atoms were added in idealized positions in a riding model following their unequivocal location in successive difference Fourier maps. Finally, all five crystal structures were deposited at the Cambridge Crystallographic Data Centre (CCDC); the corresponding CCDC numbers are listed in Table 4.

2.4 Thermal analyses

Thermal analyses were conducted on all single solvent complexes prepared in this work by employing a Perkin Elmer STA6000 simultaneous thermal analyser. The complexes were isolated from their solutions using vacuum filtration and, while still under suction, washed with low-boiling petroleum ether (bp 40–60 °C) and then patted dry with folded filter paper. Data analyses were carried out by means of Perkin Elmer Pyris 13 thermal analysis software. The purge gas was high purity nitrogen, and the samples were heated from approximately 40 to 340 °C at a heating rate of 10 °C min^{-1}. Samples were placed in ceramic pans with an empty pan serving as the reference.

2.5 Synthesis of DB3 and S4

Using known methodologies (Scheme 2), **DB3** and **S4** were synthesized from 5-dibenzosuberenone (**1a**) and 9*H*-thioxanthen-9-one (**1b**), respectively. These ketones were reacted with the Grignard reagent PhMgBr to afford the alcohols **2a** and **2b**, which were then converted to their perchlorate salts (**3a** and **3b**) with 70% $HClO_4$. Two cations were subsequently linked together using either 1,3-propanediamine (**DB3**) or 1,4-butanediamine (**S4**).

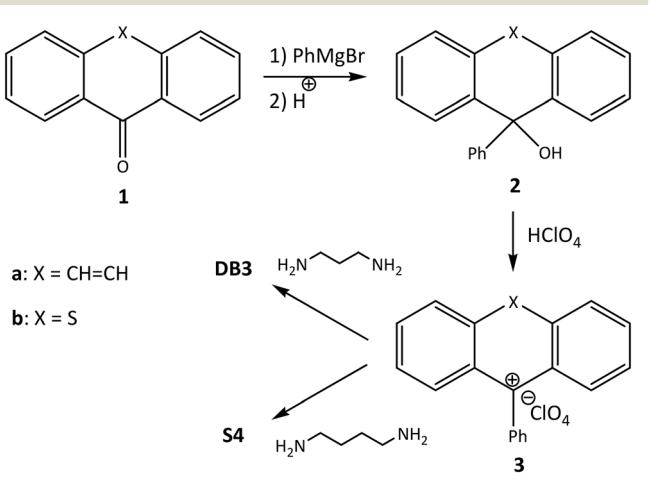

Scheme 2 The synthetic strategy towards **DB3** and **S4**.

2.5.1 Intermediates 2a and 2b, and 3a and 3b. The two alcohols (**2a** and **2b**) and perchlorate salts (**3a** and **3b**) were synthesized from **1a** and **1b**, respectively, according to reports in the literature.[29,30]

*(i) N,N′-Bis(5-phenyl-5-dibenzo[a,d]cycloheptenyl)propane-1,3-diamine (**DB3**).* The salt (**3a**, 2.01 g, 5.48 mmol) in dichloromethane (DCM, 40 mL) was added to 1,3-propanediamine (0.91 ml, 11 mmol) also in DCM (20 mL), yielding a residue which crystallized from DCM to afford *N*,*N*′-bis(5-phenyl-5-dibenzo[*a*,*d*]cycloheptenyl)propane-1,3-diamine (**DB3**) (1.49 g, 2.46 mmol, 90%) as a white solid, mp 245–248 °C (decomp.); ν_{max} (solid)/cm^{-1} 3315 (sharp, NH), and 1596 (Ar); δ_H($CDCl_3$)/ppm 1.84 (2H, appears as a singlet, NHCH$_2$C$\underline{H}_2$CH$_2$NH), 2.13 (2H, br s, N$\underline{H}$), 2.34 (4H, appears as a singlet, NHC$\underline{H}_2$CH$_2$C$\underline{H}_2$NH), 6.53 (4H, d, *J* 7.6 Hz, Ar$\underline{H}$), 6.70 (4H, s, C$\underline{H}$═C$\underline{H}$ in the B ring), 7.03 (4H, t, *J* 7.2 Hz, Ar$\underline{H}$), 7.12 (2H, t, *J* 7.2 Hz, Ar$\underline{H}$), 7.25–7.37 (8H, m, Ar$\underline{H}$), 7.46 (4H, t, *J* 7.2 Hz, Ar$\underline{H}$) and 8.00 (4H, d, *J* 7.6 Hz, Ar$\underline{H}$); δ_C($CDCl_3$)/ppm 31.2 (CH$_2$$\underline{C}H_2CH_2$), 42.3 (NH$\underline{C}H_2$), 67.7 (Ar$\underline{C}$NH), 124.7 (Ar$\underline{C}$), 125.85 (Ar$\underline{C}$), 125.90 (Ar$\underline{C}$), 126.7 (Ar$\underline{C}$), 127.4 (Ar$\underline{C}$), 128.1 (Ar$\underline{C}$), 128.9 (C$\underline{H}$═C$\underline{H}$), 131.3 (Ar$\underline{C}$), 134.4 (quaternary Ar$\underline{C}$), 141.8 (quaternary Ar$\underline{C}$) and 144.5 (quaternary Ar$\underline{C}$) [found: C, 89.0; H, 6.2; N, 4.7. $C_{45}H_{38}N_2$ requires C, 89.1; H, 6.3; N, 4.6%].

*(ii) N,N′-Bis(9-phenyl-9-thioxanthenyl)butane-1,4-diamine (**S4**).* The salt (**3b**, 0.69 g, 1.9 mmol) in DCM (40 mL) was added to 1,4-butanediamine (0.33 ml, 3.7 mmol) also in DCM (20 mL) yielding a residue which crystallized from DCM to afford *N*,*N*′-bis(9-phenyl-9-thioxanthenyl)butane-1,4-diamine (**S4**) (0.47 g, 0.74 mmol, 80%) as a white solid, mp 185–189 °C (decomp.); ν_{max} (solid)/cm^{-1} 3336 (sharp, NH), and 1584 (Ar); δ_H($CDCl_3$)/ppm 1.52 (4H, appears as a broad singlet, NHCH$_2$C$\underline{H}_2$C$\underline{H}_2$CH$_2$NH), 1.97 (2H, br s, N$\underline{H}$), 2.28 (4H, appears as a broad singlet, NHC$\underline{H}_2$CH$_2$CH$_2$C$\underline{H}_2$NH) and 6.90–7.64 (26H, m, Ar); δ_C($CDCl_3$)/ppm 28.3 (NHCH$_2$$\underline{C}H_2$), 43.9 (NH$\underline{C}H_2$), 66.5 (Ar$\underline{C}$NH), 125.9 (Ar$\underline{C}$), 126.0 (Ar$\underline{C}$), 126.87 (Ar$\underline{C}$), 126.89 (Ar$\underline{C}$), 127.9 (Ar$\underline{C}$), 128.2 (Ar$\underline{C}$), 129.6 (Ar$\underline{C}$), 131.7 (quaternary Ar$\underline{C}$), 138.1 (quaternary Ar$\underline{C}$) and 145.7 (quaternary Ar$\underline{C}$) [found: C, 79.1; H, 5.6; N, 4.3; S, 10.2. $C_{42}H_{36}N_2S_2$ requires C, 79.7; H, 5.7; N, 4.4; S, 10.1%].

2.6 Crystallization of DB3 and S4 from equimolar guest mixtures

The selectivity behaviour of **DB3** and **S4** were subsequently assessed by crystallizing each one from binary/ternary/quaternary equimolar guest mixtures comprising the Cyc/MeCyc guest solvents. Therefore, in glass vials, **DB3** (0.039 g, 0.066 mmol) or **S4** (0.041 g, 0.063 mmol) was dissolved in the equimolar guest solution (5 mmol combined amount). The vials were sealed and stored at 8 °C, and the crystals that formed in this manner were collected under suction, washed with low-boiling petroleum ether (bp 40–60 °C) and analysed by means of ^{1}H-NMR spectroscopy (for the overall host : guest (H : G) ratios) and GC (for quantification of the guest species in the mixed complexes).

2.7 Crystallization of DB3 from varying molar concentrations of binary guest mixtures

The selectivity behaviour of host compound **DB3** (0.042 g, 0.066 mmol) was further investigated by means of crystallization experiments from binary mixtures of Cyc/MeCyc, where the molar concentrations of the guests were sequentially varied to include ratios 80 : 20, 60 : 40, 40 : 60 and 20 : 80, guest A (G_A) : guest B (G_B) (5 mmol combined guest amount). The vials were again sealed and stored at 8 °C and, once the solids had formed, these were isolated and treated as in the equimolar guest experiments. Analysis was by means of GC experiments. Selectivity plots were then prepared by plotting the molar concentration of G_A or G_B in the crystals (Z_{G_A} or Z_{G_B}) against its concentration in the original solution (X_{G_A} or X_{G_B}). The selectivity coefficient (K) may be calculated using the equation $X_{G_A:G_B} = Z_{G_A}/Z_{G_B} \times X_{G_B}/X_{G_A}$, where $X_{G_A} + X_{G_B} = 1$.[31] This coefficient demonstrates the selectivity of the host species for a particular guest solvent in these mixtures. A diagonal straight line was also added to each plot to represent an unselective host compound ($X_{G_A:G_B} = 1$). For efficient practical applications, K is required to be 10 or greater.[32]

2.8 Software

All of the host–guest packing illustrations, as well as unit cell and void diagrams, were prepared using program Mercury.[33] The guests were deleted from the packing calculations for the void diagrams, and the remaining spaces analysed by means of a probe with a radius of 1.2 Å. Furthermore, stereoscopic views were prepared by employing both programs X-Seed[28] and POV-Ray.[34] Finally, Hirshfeld surface analyses were also considered by employing Crystal Explorer version 21.5.[35,36]

3. Results and discussion

3.1 Assessment of the host ability of DB3 and S4 for Cyc and the MeCycs in single solvent crystallization experiments

Table 1 contains the H : G ratios obtained after ^{1}H-NMR analyses on the solids emanating from crystallization experiments of **DB3** and **S4** from each of Cyc, 2MeCyc, 3MeCyc and 4MeCyc. While **DB3** formed 1 : 1 H : G

Table 1 Complexes formed by **DB3** and **S4** with Cyc and the MeCycs[a]

Guest	**DB3** : G ratio	**S4** : G ratio
Cyc	1 : 1	1 : 0
2MeCyc	1 : 1	1 : 0
3MeCyc	1 : 1	[b]
4MeCyc	1 : 1	1 : 1

[a] H : G ratios were determined by means of ^{1}H-NMR spectroscopy. [b] This experiment afforded a gel and no crystallization occurred.

complexes with each of these organic solvents, **S4** only included 4MeCyc, also with a 1 : 1 ratio. Neither Cyc nor 2MeCyc were complexed in this fashion, while the experiment with 3MeCyc resulted in a gel only, and no crystallization occurred (Fig. S1a–e in the ESI† contain the applicable ^{1}H-NMR spectra).

3.2 Equimolar guest competition experiments

Since both **DB3** and **S4** possessed host ability for at least some (or all) of the guest solvents in the equimolar experiments (Table 1), each one was subjected to crystallization experiments from equimolar mixed guest solutions comprising all possible guest combinations (binary/ternary/quaternary) in order to observe any host selectivity behaviour. Analysis was, once more, by means of GC experiments.

In the case of **S4**, while soluble in these solutions, crystal growth was either extremely slow (months) or no crystallization occurred at all and gels remained behind in the vials. Plausibly, this may be as a direct consequence of the fact that only 4MeCyc was complexed by this host compound in the single solvent investigations (Table 1). Therefore, these experiments were ultimately disregarded. However, **DB3** fared significantly better, and Table 2 contains a summary of the results that were obtained in this way for this host species. Experiments were conducted in duplicate to ensure their repeatability, and percentage estimated standard deviations (% e.s.d.s) are thus also presented in this table. Favoured guests in each experiment are in bold text.

Table 2 Complexes formed by **DB3** in equimolar mixed guest solutions[a]

Cyc	2MeCyc	3MeCyc	4MeCyc	Guest ratios[b] (% e.s.d.s)
X	X			**71.2** : 22.8 (1.6)
X		X		**76.4** : 23.6 (0.1)
X			**X**	42.4 : **57.6** (2.9)
	X	**X**		47.1 : **52.9** (1.8)
	X		**X**	41.1 : **58.9** (0.4)
		X	**X**	32.3 : **67.7** (1.1)
X	X	X		**61.1** : 23.6 : 15.3 (0.3) (0.2) (0.5)
X	X		X	**51.8** : 18.6 : 29.6 (2.2) (4.3) (2.1)
X		X	**X**	40.1 : 15.6 : **44.3** (2.3) (2.9) (0.9)
	X	X	**X**	30.7 : 22.9 : **46.4** (1.2) (0.9) (0.3)
X	X	X	**X**	15.4 : 26.9 : 19.2 : **38.5** (1.2) (0.6) (0.2) (0.4)

[a] Each experiment was conducted in duplicate, and the % e.s.d.s are in parentheses. [b] G : G and overall H : G ratios were obtained by employing GC and ^{1}H-NMR experiments, respectively.

There was a marked preference for 4MeCyc when **DB3** was crystallized from the equimolar binary MeCyc mixtures, with 67.7% being the highest selectivity observed (in the 3MeCyc/4MeCyc experiment) (Table 2). In those binary mixtures without 4MeCyc present, Cyc was then the favoured guest solvent (71.2 and 76.4% Cyc were measured in the Cyc/2MeCyc and Cyc/3MeCyc experiments, respectively), while an absence of both 4MeCyc and Cyc then saw more of 3MeCyc being complexed (2MeCyc/3MeCyc, 52.9% 3MeCyc). Interestingly, the host affinity in the ternary mixtures was towards Cyc when the solutions contained Cyc/2MeCyc/3MeCyc (61.1%) and Cyc/2MeCyc/4MeCyc (51.8%), while 4MeCyc was preferred in the Cyc/3MeCyc/4MeCyc (44.3%) and 2MeCyc/3MeCyc/4MeCyc (46.4%) experiments. The quaternary solvent, once more, revealed a host affinity towards 4MeCyc (38.5%).

Overall, it is clear from the data contained in Table 2 that 4MeCyc and Cyc were more usually favoured compared with 3MeCyc and 2MeCyc, with the latter guest solvent never being a preferred guest of **DB3** (all of the GC traces for these experiments have been provided in the ESI,† Fig. S2–S4).

3.3 Non-equimolar binary guest competition experiments

As was the case in the equimolar guest competition experiments with **S4**, crystal growth, if at all, was slow in the binary non-equimolar guest experiments, and these were thus also disregarded in this particular instance. Once more, **DB3** worked effectively in these experimental conditions and the results thus obtained are discussed now.

In Cyc/2MeCyc solutions (Fig. 1a), **DB3** possessed a distinct preference for Cyc in all cases, except when the solution contained 80% 2MeCyc, when 2MeCyc was then the favoured solvent. All K values, however, were low (2 or less) and so separations of these binary mixtures through host–guest chemistry are not feasible. Similar observations were made in the Cyc/3MeCyc solutions (Fig. 1b): Cyc was preferred when its concentration in the solution exceeded 20%, while 3MeCyc was favoured in the 20 : 80 Cyc/3MeCyc solution. Again, K values were not significant (3.2–3.9 for experiments in favour of Cyc), and **DB3** is not a likely host candidate for these separations. From Fig. 1c (4MeCyc/Cyc), the host compound was, for all intents and purposes, unselective, the experimentally obtained data points approaching the diagonal straight line representing an unselective host compound (K = 1). This was also the case for the 2MeCyc/3MeCyc experiments (Fig. 1d). Finally, the 4MeCyc/2MeCyc and 4MeCyc/3MeCyc guest combinations (Fig. 1e and f) provided selectivity profiles that describe a consistent preference for 4MeCyc across the concentration range. However, the K values remained low (1.4–2.2).

In summary, none of these binary mixtures can be effectively separated using **DB3** as the host compound (all of the calculated K values in this investigation may be

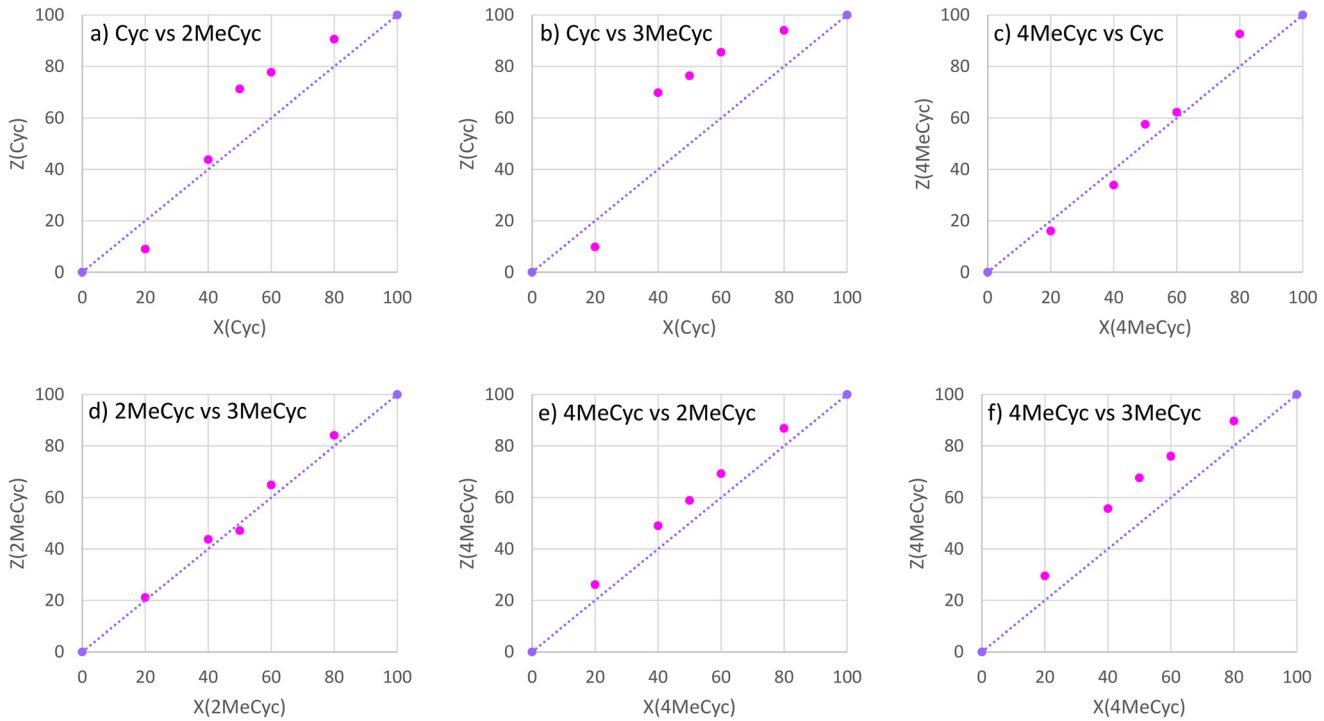

Fig. 1 Selectivity profiles for a) Cyc/2MeCyc, b) Cyc/3MeCyc, c) 4MeCyc/Cyc, d) 2MeCyc/3MeCyc, e) 4MeCyc/2MeCyc and f) 4MeCyc/3MeCyc binary solutions with **DB3** as the host compound.

Table 3 Crystallographic parameters for the complexes of **DB3** and **S4** with the cyclohexanones

	DB3·Cyc	**DB3**·2MeCyc	**DB3**·3MeCyc	**DB3**·4MeCyc	**S4**·4MeCyc
Chemical formula	$C_{45}H_{38}N_2{\cdot}C_6H_{10}O$	$C_{45}H_{38}N_2{\cdot}C_7H_{12}O$	$C_{45}H_{38}N_2{\cdot}C_7H_{12}O$	$C_{45}H_{38}N_2{\cdot}C_7H_{12}O$	$C_{42}H_{36}N_2S_2{\cdot}C_7H_{12}O$
Formula weight	704.91	718.94	718.94	718.94	745.01
Crystal system	Orthorhombic	Triclinic	Triclinic	Triclinic	Triclinic
Space group	$Pna2_1$	$P\bar{1}$	$P\bar{1}$	$P\bar{1}$	$P\bar{1}$
μ(MoKα)/mm^{-1}	0.073	0.072	0.072	0.072	0.178
a/Å	15.1599(10)	8.7792(13)	8.8102(7)	8.8224(6)	9.2379(5)
b/Å	11.4773(6)	15.350(2)	15.3893(11)	15.4017(11)	9.5888(5)
c/Å	21.8168(14)	15.553(2)	15.4064(12)	15.5782(11)	12.5881(7)
Alpha/°	90	98.013(5)	99.086(2)	98.682(2)	93.280(2)
Beta/°	90	105.903(5)	102.942(2)	104.994(2)	101.236(2)
Gamma/°	90	101.393(5)	101.262(2)	102.791(2)	115.9147(19)
V/Å^3	3796.0(4)	1933.9(5)	1951.6(3)	1944.6(2)	970.82(9)
Z	4	2	2	2	1
D(calc)/g cm^{-3}	1.233	1.235	1.223	1.228	1.274
F(000)	1504	768	768	768	396
Temp./K	100	100	100	100	200
Restraints	1	2	48	0	60
N_{ref}	8391	7149	8636	9727	4807
N_{par}	495	270	579	505	280
R	0.0540	0.1641	0.0621	0.0537	0.0667
wR_2	0.1350	0.2969	0.1246	0.1114	0.1439
S	1.05	1.23	1.02	1.09	1.19
θ min–max/°	2.2, 27.2	2.2, 25.5	2.2, 27.2	2.2, 28.4	2.4, 28.3
Tot. data	90 743	86 445	56 222	98 665	56 887
Unique data	8391	7149	8636	9727	4807
Observed data [$I > 2.0$ sigma(I)]	7864	5906	5033	8151	4005
R_{int}	0.061	0.198	0.122	0.072	0.077
Completeness	0.996	0.999	0.999	0.999	0.999
Min. resd. dens. (e Å^{-3})	−0.29	−0.49	−0.33	−0.25	−0.32
Max. resd. dens. (e Å^{-3})	0.55	0.70	0.46	0.35	0.55
CCDC number	2349323	2338004	2338003	2338005	2429121

found in the ESI,† Table S1, as well as all the applicable GC traces, Fig. S5–S10).

3.4 SCXRD analysis on inclusion compounds with DB3 and S4

Table 3 contains a summary of the relevant crystallographic parameters used to obtain the crystal structures for the five complexes reported in the present investigation. While **DB3**·Cyc was solved in the orthorhombic crystal system and space group $Pna2_1$, the remaining complexes all crystallized in the triclinic crystal system, the space group being consistently $P\bar{1}$.

In the 2MeCyc complex with **DB3** was observed persistent multiple twinning of the crystals of this phase, which required an extremely low volume crystal for data-collection. Despite the compromised data, the structure was solved and is unambiguous; however, R_1 (0.1641) and wR_2 (0.2969) are abnormally high as a

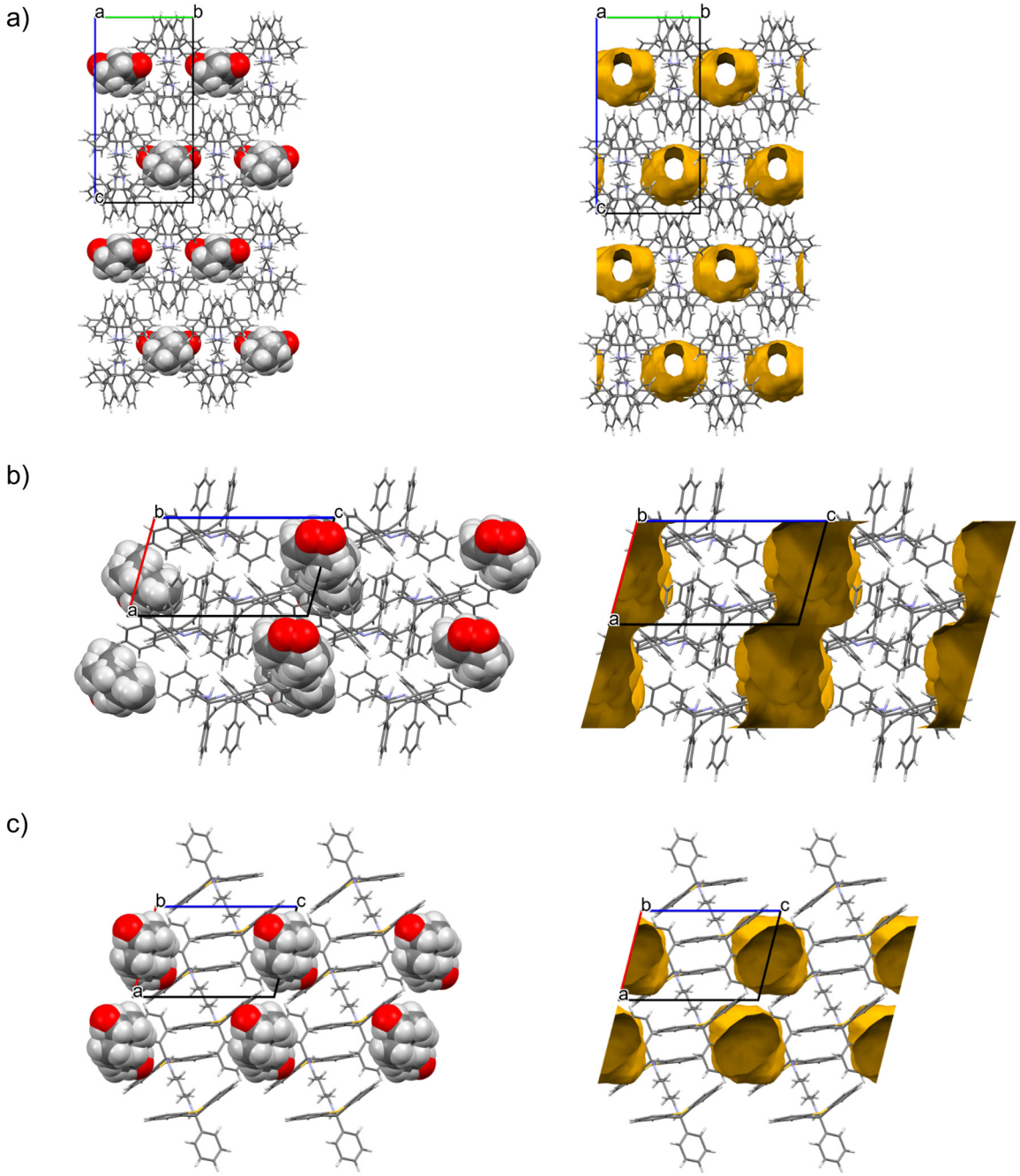

Fig. 2 Unit cell and host–guest packing (left) and void (right) diagrams for a) **DB3**·Cyc [100], b) **DB3**·3MeCyc [010] (representing also **DB3**·2MeCyc and **DB3**·4MeCyc) and c) **S4**·4MeCyc [010]. All host species are represented in stick form while guest molecules are in space-filling representation.

result. The thermal displacement parameters U_{iso} for the non-hydrogen atoms of the host molecule were abnormally low and their attempted anisotropic refinement led to numerous non-positive definite indications, resulting in the need to revert to isotropic refinement. However, the U_{iso} values of the atoms of the guest molecule were normal and their subsequent anisotropic refinement was possible.

When the 3MeCyc-containing complex with this host compound was solved, it was observed that the guest molecule occupied two alternative positions with site occupancy factors (s.o.f.s) of 0.76 and 0.24; however, this disorder was successfully modelled, the atoms of the minor component being refined anisotropically with the ISOR restraint. In **S4**·4MeCyc, the guest molecule was disordered around an inversion centre. Finally, the Cyc- and 4-MeCyc-containing inclusion compounds with **DB3** displayed no disorder whatsoever.

The unit cell parameters for the MeCyc complexes with **DB3** are all very similar, suggesting the possibility of a common host packing arrangement. Program Mercury was used to calculate the three PXRD patterns (Fig. S11†) whose close resemblance with respect to both peak angular positions and relative peak intensities confirmed the isostructurality. This packing arrangement differed in **S4**·4MeCyc and **DB3**·Cyc.

The guest accommodation type was investigated in the complexes containing the four cyclohexanones with **DB3** by removing the guests from the packing calculations: all guests were located in endless channels, but these were extremely constricted in the case of **DB3**·Cyc (Fig. 2a and b, where the latter figure, for **DB3**·3MeCyc, also represents **DB3**·2MeCyc and **DB3**·4MeCyc, due to the observed isostructurality of the three complexes). The accommodation of 4MeCyc in its complex with **S4** was in the form of discrete cavities (Fig. 2c).

From the crystal structures of the complexes of **DB3**, the host molecule assumed a bowl-like conformation owing to the folded diamino linker unit. Upon superimposing the CH_2 carbon atoms directly attached to each nitrogen atom, it was noted that the two C–N bonds in **DB3**·Cyc were oriented at almost 90° with respect to one another, while these were, in the three isostructural complexes, almost superimposed. The angles between the planes of the free aromatic moieties measured 68.8(2)° in the Cyc-containing complex, and 83.2(3), 83.7(1) and 82.7(1)° in those with 2MeCyc, 3MeCyc and 4MeCyc (these being comparable owing to the isostructurality evident in these three complexes). Fig. 3a and b are depictions of these planes in **DB3**·Cyc and **DB3**·2MeCyc (representing also the complexes with 3MeCyc and 4MeCyc), while Fig. 4a–c are stereoscopic views of the host molecule conformations in **DB3**·Cyc, **DB3**·2MeCyc (once more, representing the isostructural complexes) and **S4**·4MeCyc, respectively.

The structure of the host molecule in the **S4** complex with 4MeCyc is unique, the butane-1,4-diamine chain displaying an extended conformation, which is consistent with the requirement of the location of the host molecule on an inversion centre, since $Z = 1$ in the space group $P\bar{1}$.

Only in **DB3**·Cyc was observed an intermolecular π···π interaction between two neighbouring host molecules (Fig. 5) with a Cg···Cg distance that measured 3.654(2) Å with a slippage of 0.930 Å; this type of interaction was not present in any of the remaining complexes (of **DB3** and **S4**).

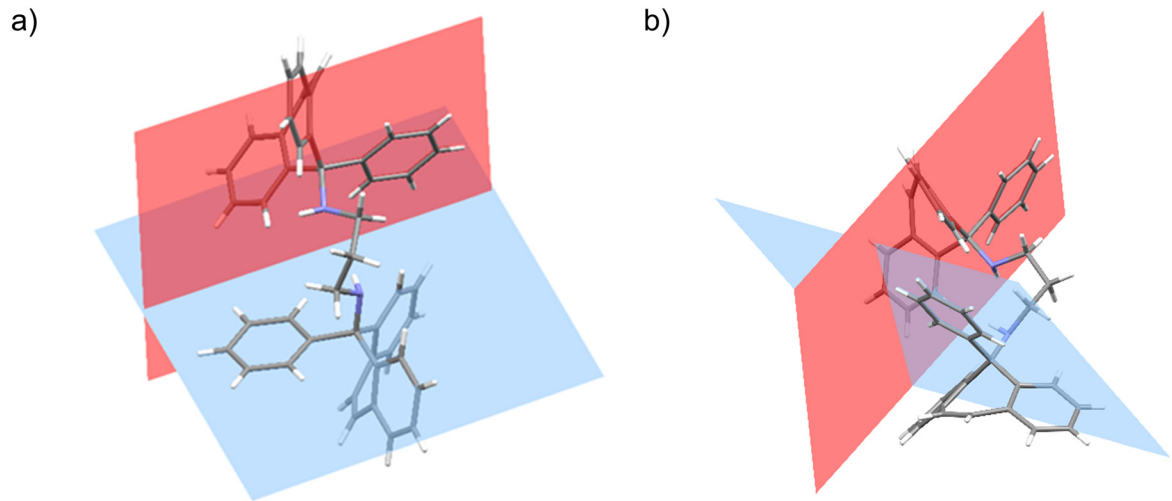

Fig. 3 Calculated least-squares planes of the free aromatic rings in a) **DB3**·Cyc and b) **DB3**·2MeCyc (representing also **DB3**·3MeCyc and **DB3**·4MeCyc); guest molecules have been deleted.

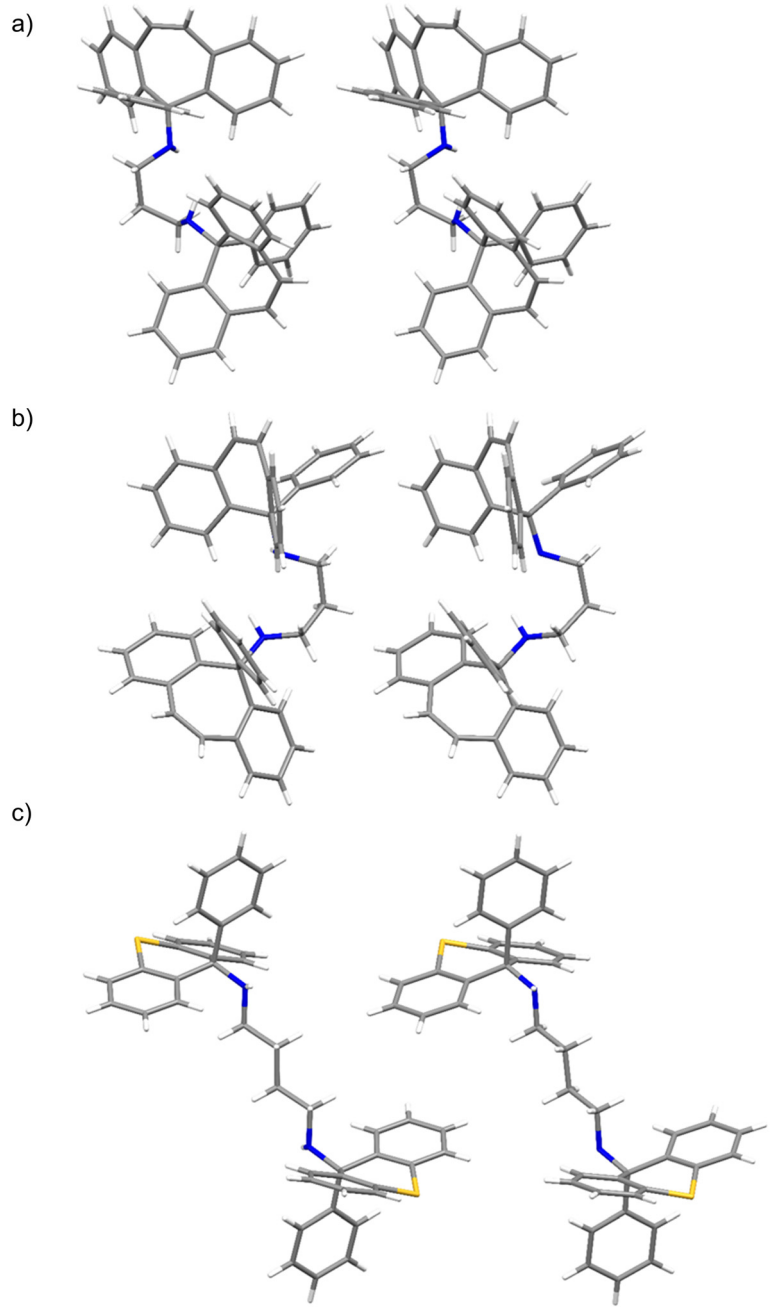

Fig. 4 Stereoviews depicting the conformations of the host molecules in a) **DB3**·Cyc, b) **DB3**·2MeCyc (as representative of the three isostructural cases) and c) **S4**·4MeCyc; guest molecules have been deleted.

Table 4 summarises the various parameters of the C–H···π bonds that were identified in the five complexes. These were both inter- and intramolecular in nature, and were observed within host molecules (between the aromatic hydrogens of the tricyclic fused system and the free aromatic ring moieties), between them and, additionally, between host and guest species, and ranged between 2.64–2.95 (H···π) and 3.491(4)–3.907(10) Å, with accompanying angles between 127 and 168°. Interestingly, in **DB3**·Cyc, interactions of this type were not evident between the host and guest molecules nor within each host molecule, while one or more of these types of contacts were observed in the remaining four complexes. The reason for the absence of intramolecular (host)C–H···π(host) interactions in **DB3**·Cyc is unclear, but it is plausible that the unique conformation of the diamino linker of this host molecule in this complex impedes an

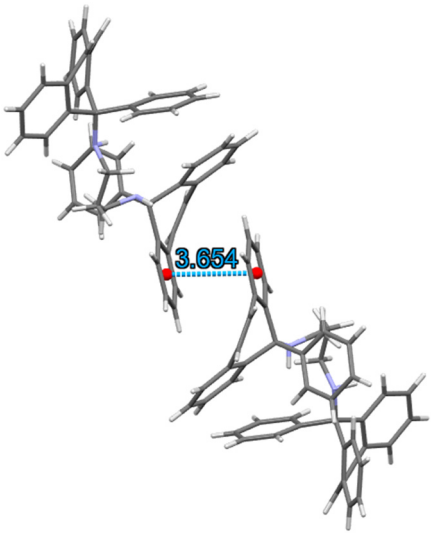

Fig. 5 The π···π stacking interaction between two host molecules in the **DB3**·Cyc complex.

intramolecular contact of this kind, since the linker conformation causes the dibenzo[*a*,*d*]cycloheptenyl aromatic hydrogen atoms to tilt away from the free phenyl rings.

Only **DB3**·Cyc, having a preferred guest species, displayed a classical hydrogen bond between the host and guest molecules (Fig. 6, a stereoscopic view); interaction parameters were 2.44(3) Å (H···O) and 3.350(4) Å (N···O), with a nearly linear (173(3)°) N–H···O bond angle. The remaining interactions were non-classical and intermolecular in nature (except in **DB3**·Cyc where these were not observed): one such contact was identified in **DB3**·2MeCyc between the hydrogen atom of the dibenzo[*a*,*d*]cycloheptenyl moiety and the oxygen atom of 2MeCyc (2.59 Å (H···O), 3.419(10) Å (C···O) and 146° (C–H···O)), one in **DB3**·3MeCyc and two in **DB3**·4MeCyc (2.54 Å (H···O), 3.398(15) Å (C···O), 151° (C–H···O), and 2.67, 2.70 Å (H···O), 3.761, 3.562 Å (C···O), 165, 151° (C–H···O), respectively). These kinds of interactions were also observed between guest molecules in the complex **DB3**·4MeCyc (2.56 Å, 3.331(2) Å and 135°). In **S4**·4MeCyc, this close contact was between the thioxanthenyl aromatic hydrogen atom and the oxygen atom of the guest molecule (2.71 Å, 3.602 Å and 157°).

Table 5 (where A is the acceptor and D the donor atoms) contains a summary of all of the intramolecular hydrogen bonds identified in the five complexes. These were only non-classical in nature in **DB3**·Cyc and **S4**·4MeCyc, while classical hydrogen bonding interactions

Table 4 Parameters of the C–H···π bonds in the five complexes

	Interaction	H···π/Å	C–H···π/°	C···π/Å
DB3·Cyc	(Host)C–H···π(host)[b]	2.68	155	3.565(4)
	(Host)C–H···π(host)[b]	2.64	149	3.491(4)
DB3·2MeCyc	(Host)C–H···π(host)[a]	2.92	128	3.608(7)
	(Guest)C–H···π(host)[b]	2.95	163	3.907(10)
DB3·3MeCyc	(Host)C–H···π(host)[a]	2.94	128	3.628(2)
	(Guest)C–H···π(host)[b]	2.85	155	3.763(11)
DB3·4MeCyc	(Host)C–H···π(host)[a]	2.92	127	3.605(2)
	(Guest)C–H···π(host)[b]	2.88	145	3.733(2)
	(Guest)C–H···π(host)[b]	2.87	168	3.836(2)
S4·4MeCyc	(Host)C–H···π(host)[a]	2.83	134	3.560(3)
	(Guest)C–H···π(host)[b,c]	2.90	151	3.792(8)

[a] Intramolecular. [b] Intermolecular. [c] This guest interaction involved the second guest disorder component.

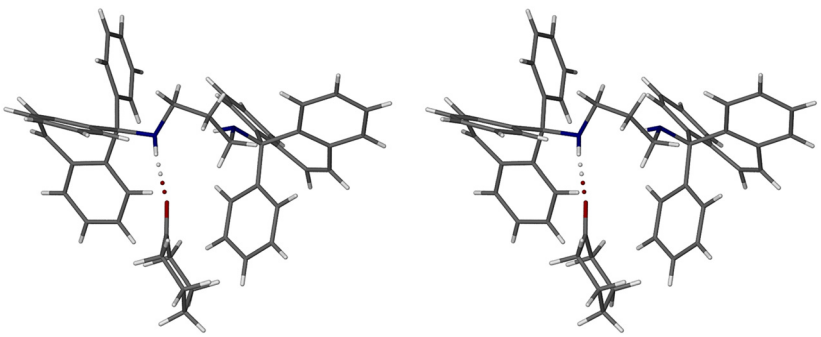

Fig. 6 Stereoview depicting the (host)N–H···O(guest) classical hydrogen bond in **DB3**·Cyc.

Table 5 Intramolecular hydrogen bonding short contacts in the complexes of **DB3** and **S4**

Complex		H···A/Å	D···A/Å	D–H···A/°
	Classical H-bonds			
DB3·Cyc	None			
DB3·2MeCyc	N–H···N	2.46(6)	3.053(7)	126(6)
DB3·3MeCyc	N–H···N	2.32(3)	3.059(3)	133(2)
DB3·4MeCyc	N–H···N	2.39(2)	3.061(2)	132(2)
S4·4MeCyc	None			
	Non-classical H-bonds			
DB3·Cyc	C–H···N	2.46, 2.32	2.846(4), 2.710(4)	All 104
DB3·2MeCyc	C–H···N	2.37, 2.38	2.752(4), 2.762(4)	104, 103
		2.33, 2.47	2.715(8), 2.835(9)	104, 103
DB3·3MeCyc	C–H···N	2.36, 2.41	2.742(3), 2.793(3)	104, 104
		2.34, 2.41	2.724(3), 2.789(3)	103, 103
DB3·4MeCyc	C–H···N	2.35, 2.41	2.726(3), 2.785(3)	104, 103
		2.35, 2.43	2.7378(19), 2.802(2)	104, 104
S4·4MeCyc	C–H···N	2.34, 2.41	2.7274(19), 2.793(2)	All 102
		2.48, 2.46	2.839(3), 2.807(3)	

were observed in the **DB3** complexes with the MeCycs, where the hydrogen atom of the N–H group of the diamino linker interacted with the second N atom of the same linker (H···N measured 2.32(2)–2.46(6) Å, N···N 3.053(7)–3.061(2) Å and N–H···N 126(6)–133(2)°). The non-classical intramolecular hydrogen bonds were pervasive, being identified in all five complexes, and H···N distances were between 2.32 and 2.48 Å (2.710(4)–2.846(3) Å, 102–104°).

3.5 Hirshfeld surface analysis

The intermolecular host···guest interactions for the **DB3** complexes were further quantified by employing Hirshfeld surface analyses[35,36] (these analyses were not carried out on **S4**·4MeCyc since this was the only complex of **S4** and comparisons were thus not possible). At the outset, three-dimensional (3D) surfaces were generated around the guest molecules using program Crystal Explorer version 21.5. These surfaces were then converted into two-dimensional (2D) fingerprint plots which illustrate the distances between the guest atom within the surface (d_i) and the nearest host atom on the outside of it (d_e). Due to the disorder in the guest molecule in **DB3**·3MeCyc, each disordered guest component was investigated in turn. Fig. 7 illustrates both the Hirshfeld 3D surfaces and the associated 2D fingerprint plots, where numbers "1" relate to the 'spikes' on these plots owing to (guest) O···H(host) interactions, and "2" and "3" are the 'wings' signifying the (guest)C···H(host) and (guest)H···H(host) interactions, respectively.

Fig. 8 shows the quantity of the different interactions present between the host and guest molecules in the **DB3** complexes by means of a bar graph. It is evident from this figure that there were no significant (guest)C···C(host) contacts. Furthermore, only **DB3**·Cyc (having a favoured guest species) demonstrated (guest)H···N(host) interactions but the percentage was low (0.2%). Interestingly, unsubstituted Cyc, despite only having 10 hydrogen atoms, was involved in the greatest amount (79.3%) of (guest) H···H(host) interactions (these interactions for the isomeric MeCycs bearing 12 hydrogen atoms ranged between only 61.5 and 66.6%).

3.6 Thermal analysis

Thermal analysis was carried out on the four complexes of **DB3** in order to determine their relative thermal stabilities by considering the temperatures at which the guest release event commenced (T_{on}). The **S4**·4MeCyc was also analysed in this manner for completeness. The thermogravimetric (TG, red) and its derivative (DTG, purple) as well as the differential scanning calorimetry (DSC, blue) plots are provided in Fig. 9a–e for the five complexes and a summary of the data they provide may be found in Table 6.

The expected and experimental mass losses for the guest release event concurred closely (calculated losses 13.9, 15.6, 15.6, 15.6, 15.1% compared with the experimental losses 14.2, 14.7, 15.6, 16.0, 13.5 for **DB3**·Cyc, **DB3**·2MeCyc, **DB3**·3MeCyc, **DB3**·4MeCyc and **S4**·4MeCyc) (Table 6).

The guest loss events for the **DB3** complexes were single stepped, while that for **S4**·4MeCyc occurred in two broad steps.

From the T_{on} data contained in this table, of the four **DB3** complexes, **DB3**·Cyc was the most stable one, decomposing at 134.2 °C. This may explain why Cyc was one of the preferred guests of **DB3** in the guest competition experiments. Furthermore, since SCXRD analyses demonstrated that only Cyc formed a classical hydrogen bond with the host molecule, the **DB3**·Cyc complex is

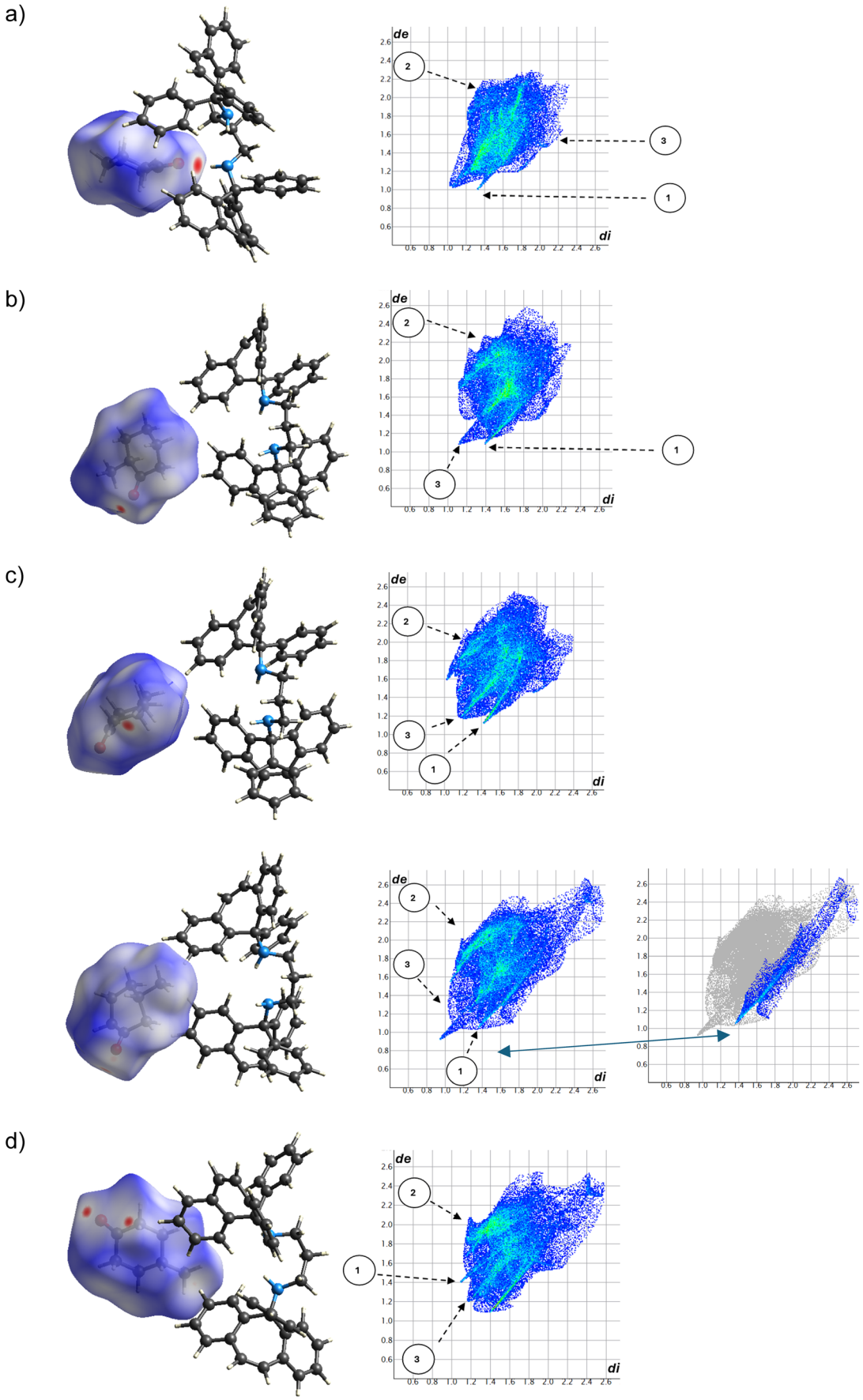

Fig. 7 Hirshfeld surfaces (left) and 2D fingerprint plots (right) for complexes a) **DB3**·Cyc, b) **DB3**·2MeCyc, c) **DB3**·3MeCyc (disorder guest component 1 (top) and 2 (bottom)), and d) **DB3**·4MeCyc. In the case of the bottom 2D plot for **DB3**·3MeCyc, the spike for 1 was unclear and therefore a second image was added for clarity (right).

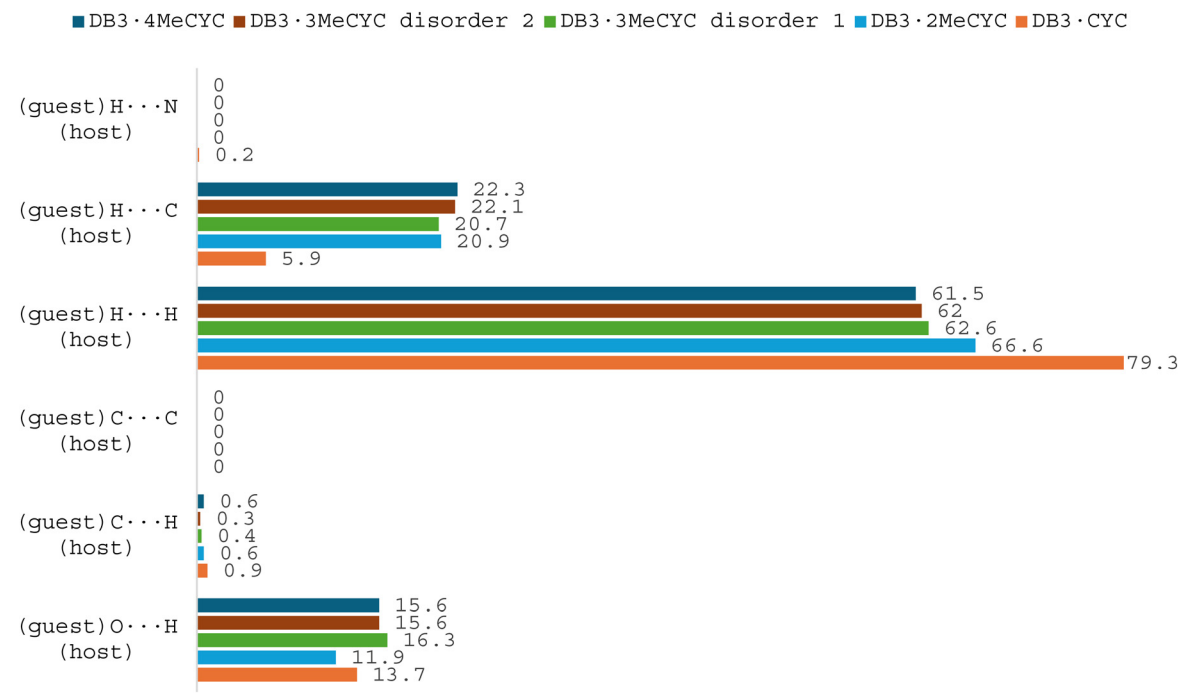

Fig. 8 Quantification of all of the guest···host interactions in the **DB3** complexes.

expected to possess the greater thermal stability. To add to this, Cyc occupied channels that were extremely constricted compared with the MeCyc-containing complexes, where the guests were located in wide open channels: this additionally explains why **DB3**·Cyc was the most stable of the four. While these data do not explain why the affinity of the host compound for 4MeCyc was so overwhelming, it does indeed provide an explanation for the low host selectivity for 2MeCyc and 3MeCyc.

4. Conclusions

In this work, host compounds **DB3** and **S4** were designed to have both hydrogen-bonding ability (NH groups) and bulky aromatics that may serve to surround potential guest molecules in any successfully formed inclusion compounds. These two compounds were then effectively synthesized through, initially, a Grignard addition reaction on suitable ketones, followed by treatment of the resultant alcohols with perchloric acid. Two perchlorate salt moieties were then linked together through reaction with diamino-substituted alkanes. Compound **DB3** was demonstrated to have the ability to enclathrate each of Cyc, 2MeCyc, 3MeCyc and 4MeCyc, all with 1:1 H:G ratios, while **S4** only included 4MeCyc, also with a 1:1 ratio. In mixed guest competition experiments, **DB3** showed an overwhelming affinity for 4MeCyc and then Cyc, more usually disfavouring 3MeCyc and 2MeCyc. However, this host compound is not an appropriate candidate for the separations of mixtures of these cyclohexanones through host–guest chemistry strategies owing to the low selectivity coefficients that were calculated in the binary guest mixture experiments. In analogous conditions, the crystal growth of **S4** was extremely slow and hence not practical for such separations, and so this host compound was disregarded in further guest competition experiments. However, despite these drawbacks, the crystal structures of the five novel complexes synthesized here were subjected to an in-depth scrutiny through SCXRD experiments. Cyc, a preferred guest solvent of **DB3**, occupied highly constricted channels in the crystals of the complex while the accommodation of the MeCycs was in wider and more open channels. Additionally, only Cyc engaged in a classical hydrogen bond with **DB3**. Hirshfeld surface analyses demonstrated that in **DB3**·Cyc, despite Cyc having less hydrogen atoms, this guest species was involved in a greater quantity of (guest)H···H(host) interactions compared with the MeCycs, despite these isomers having a greater number of hydrogen atoms. These observations explain the host affinity behaviour for Cyc (but not for 4MeCyc). The geometries of the diamino linkers in the complexes were also analysed and it was observed that this chain in **DB3** assumed a more folded conformation, while this linker in **S4**·4MeCyc presented in an extended zig-zag form. Thermal analyses concurred with observations made in the guest competition experiments in that **DB3**·Cyc was a more stable complex of this host compound but, once more, the host affinity for, also, 4MeCyc could not be clarified by means of this technique.

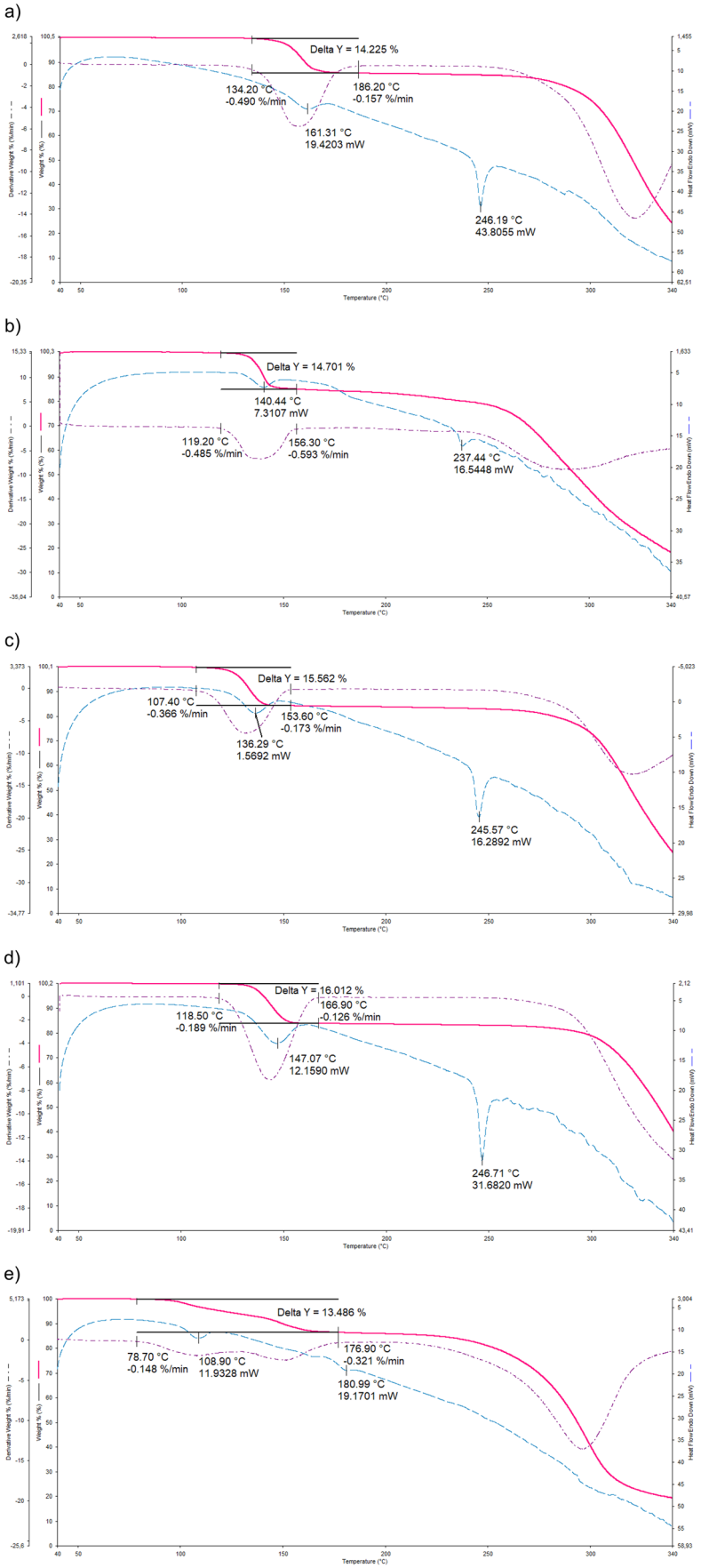

Fig. 9 Overlaid TG, DTG and DSC traces for a) **DB3**·Cyc, b) **DB3**·2MeCyc, c) **DB3**·3MeCyc, d) **DB3**·4MeCyc and e) **S4**·4MeCyc.

Table 6 Thermal data obtained from the DSC, TG and DTG plots for the five complexes

Complex	T_{on}[a]/°C	Calculated mass loss/%	Experimental mass loss/%
DB3·Cyc	134.2	13.9	14.2
DB3·2MeCyc	119.2	15.6	14.7
DB3·3MeCyc	107.4	15.6	15.6
DB3·4MeCyc	118.5	15.6	16.0
S4·4MeCyc	78.7	15.1	13.5

[a] T_{on}, the onset temperature for the guest release process, is a measure of the relative thermal stability of the complex.

Data availability

The crystal structures of complexes **DB3**·Cyc, **DB3**·2MeCyc, **DB3**·3MeCyc, **DB3**·4MeCyc and **S4**·4MeCyc were deposited at the Cambridge Crystallographic Data Centre (CCDC) and their CCDC numbers are 2349323, 2338004, 2338003, 2338005 and 2429121, respectively.

Author contributions

D. B. T.: investigation; methodology; validation; writing the original draft. B. B.: conceptualization; funding acquisition; methodology; project administration; resources; supervision; visualization; assistance with editing the original draft. M. R. C.: resources; assistance with editing the second draft; data curation; formal analysis. E. C. H.: data curation; formal analysis.

Conflicts of interest

There are no conflicts of interest to declare.

Acknowledgements

Financial support is acknowledged from the Nelson Mandela University, and B. B. also thanks the National Research Foundation (South Africa) as does D. B. T. (NRF grant number PMDS22052414135). M. R. C. thanks the University of Cape Town for access to research facilities in the Department of Chemistry.

References

1 Cyclohexanone; MSDS No. ARK2189 [Online], Merck Life Science (Pty) Ltd., Modderfontein, SA, March 01, 2024, **https://www.sigmaaldrich.com/ZA/en/sds/sial/ark2189?userType=anonymous**, [Accessed 18/04/2024].

2 2-Methylcyclohexanone MSDS No. M38400 [Online], Merck Life Science (Pty) Ltd., Modderfontein, SA, February 24, 2023, **https://www.sigmaaldrich.com/ZA/en/sds/aldrich/m38400?userType=anonymous**, [Accessed 18/04/2024].

3 3-Methylcyclohexanone; MSDS No. W394718 [Online], Merck Life Science (Pty) Ltd., Modderfontein, SA, August 12, 2023, **https://www.sigmaaldrich.com/ZA/en/sds/aldrich/w394718?userType=anonymous**, [Accessed 18/04/2024].

4 4-Methylcyclohexanone; MSDS No. 173614 [Online], Merck Life Science (Pty) Ltd., Modderfontein, SA, November 02, 2023, **https://www.sigmaaldrich.com/ZA/en/sds/aldrich/173614?userType=anonymous**, [Accessed 18/04/2024].

5 K. Robards and D. Ryan, Sample handling in chromatography, in *Elsevier eBooks*, 2022, pp. 453–493, DOI: **10.1016/b978-0-12-822096-2.00007-4**.

6 Simple vs. Fractional Distillation: Which Method is Right for Your Separation Process?, **https://kindle-tech.com/faqs/what-are-the-advantages-and-disadvantages-of-simple-and-fractional-distillation?srsltid=AfmBOor3NBE0ntogxo9QHyW9NDXoMFMbCQ_VWkMdoapoF9UEPpJMUjp-**, [Accessed 25/02/2025].

7 Advantages And Limitations Of Fractional Distillation. FasterCapital, **https://fastercapital.com/topics/advantages-and-limitations-of-fractional-distillation.html**, [Accessed 25/02/2025].

8 Y. Li, Z. Liu, W. Xue, S. P. Crossley, F. C. Jentoft and S. Wang, Hydrogenation of *o*-cresol on platinum catalyst: catalytic experiments and first-principles calculations, *Appl. Surf. Sci.*, 2017, **393**, 212–220.

9 A. Romero, P. Yustos and A. Santos, Dehydrogenation of cyclohexanol to cyclohexanone: influence of methylcyclopentanols on the impurities obtained in ε-caprolactam, *Ind. Eng. Chem. Res.*, 2003, **42**, 3654–3661.

10 L. R. Nassimbeni, Physicochemical studies of separation of isomers by supramolecular systems, *Perspectives in Supramolecular Chemistry*, 2004, pp. 123–135, DOI: **10.1002/0470020261.ch5**.

11 G. W. Gokel, *Crown Ethers and Cryptands*, Royal Society of Chemistry, United Kingdom, 1991, DOI: **10.1039/9781788010917**.

12 D. Seebach, A. K. Beck and A. Heckel, TADDOLs, their derivatives, and TADDOL analogues: versatile chiral auxiliaries, *Angew. Chem., Int. Ed.*, 2001, **40**, 92–138, DOI: **10.1002/1521-3773(20010105)40:1**.

13 H. Bawa, H. Su, S. De Doncker, S. A. Bourne and L. R. Nassimbeni, Selectivity of picoline by enclathration: Structure and Kinetics of decomposition, *Cryst. Growth Des.*, 2024, **24**(20), 8550–8556, DOI: **10.1021/acs.cgd.4c01061**.

14 B. Barton, M. R. Caira, U. Senekal and E. C. Hosten, Host compounds based on the rigid 9,10-dihydro-9,10-ethanoanthracene framework: selectivity behaviour in mixed isomeric dichlorobenzenes, *CrystEngComm*, 2024, **26**, 1862–1875, DOI: **10.1039/d4ce00113c**.

15 Y. Zhao, H. Xiao, C.-H. Tung, L.-Z. Wu and H. Cong, Adsorptive separation of cyclohexanol and cyclohexanone by nonporous adaptive crystals of RhombicArene, *Chem. Sci.*, 2021, **12**, 15528–15532, DOI: **10.1039/d1sc04728k**.

16 B. Barton, S.-L. Dorfling and E. C. Hosten, Cyclohexanone-driven discriminatory behavior change of host compound (+)-(2*R*,3*R*)-TETROL for isomeric methylcyclohexanone guests, *Cryst. Growth Des.*, 2017, **17**, 6725–6732, DOI: **10.1021/acs.cgd.7b01334**.
17 B. Barton, L. De Jager, U. Senekal and E. C. Hosten, Comparing the effect of selected substituent changes on host ability and selectivity in four xanthenyl-type host compounds in the presence of cyclohexanone and methylcyclohexanone isomers, *J. Incl. Phenom. Macrocycl. Chem.*, 2019, **95**, 259–271, DOI: **10.1007/s10847-019-00941-7**.
18 E. V. Anslyn and D. A. Dougherty, *Modern physical organic chemistry*, University Science Books, 2006.
19 J. L. Atwood and J. W. Steed, *Encyclopedia of Supramolecular Chemistry*, CRC Press, 2004.
20 J. W. Steed, D. R. Turner and K. J. Wallace, *Core concepts in supramolecular chemistry and nanochemistry*, 2007.
21 Bruker, *APEX2, SADABS and SAINT*, Bruker AXS, Madison, 2010.
22 G. M. Sheldrick, SHELXT–Integrated space-group and crystal-structure determination, *Acta Crystallogr., Sect. A: Found. Adv.*, 2015, **71**, 3–8.
23 G. M. Sheldrick, Crystal structure refinement with SHELXL. Acta Crystallogr., Sect. C, *Struct. Chem.*, 2015, **71**, 3–8.
24 C. B. Hübschle, G. M. Sheldrick and B. Dittrich, ShelXle: a Qt graphical user interface for SHELXL, *J. Appl. Crystallogr.*, 2011, **44**, 1281–1284.
25 Bruker, *APEX3 v2019.1-0, SAINT V8.40A*, Bruker AXS Inc., Madison (WI), USA, 2019.
26 L. Krause, R. Herbst-Irmer, G. M. Sheldrick and D. Stalke, Comparison of silver and molybdenum microfocus X-ray sources for single-crystal structure determination, *J. Appl. Crystallogr.*, 2015, **48**, 3–10.
27 G. M. Sheldrick, A short history of SHELX, *Acta Crystallogr., Sect. A: Found. Crystallogr.*, 2008, **64**, 112–122.
28 L. J. Barbour, X-Seed–A software tool for supramolecular crystallography, *J. Supramol. Chem.*, 2001, **1**, 189–191.
29 E. Weber, N. Dörpinghaus and I. Csöregh, Versatile and convenient lattice hosts derived from singly bridged triarylmethane frameworks, X-ray crystal structures of three inclusion compounds, *J. Chem. Soc., Perkin Trans. 2*, 1990, **12**, 2167–2177, DOI: **10.1039/p29900002167**.
30 B. Taljaard, A. Goosen and C. W. McCleland, Synthesis of hydrogen peroxide: acid-catalysed decomposition of 9-hydroperoxy-9-phenylxanthene and its derivatives, *S. Afr. J. Chem.*, 1987, **40**, 139–145.
31 A. M. Pivovar, K. T. Holman and M. D. Ward, Shape-selective separation of molecular isomers with tunable hydrogen-bonded host frameworks, *Chem. Mater.*, 2001, **13**, 3018–3031, DOI: **10.1021/cm0104452**.
32 N. M. Sykes, H. Su, E. Weber, S. A. Bourne and L. R. Nassimbeni, Selective enclathration of methyl- and dimethylpiperidines by fluorenol hosts, *Cryst. Growth Des.*, 2017, **17**, 819–826.
33 C. F. Macrae, I. Sovago, S. J. Cottrell, P. T. A. Galek, P. McCabe, E. Pidcock, M. Platings, G. P. Shields, J. S. Stevens, M. Towler and P. A. Wood, Mercury 4.0: from visualization to analysis. Design and prediction, *J. Appl. Crystallogr.*, 2020, **53**, 226–235.
34 POV-Ray for Windows, Version 3.1e, The persistence of vision team, ©, 1991–1999.
35 M. A. Spackman and D. Jayatilaka, Hirshfeld surface analysis, *CrystEngComm*, 2009, **11**, 19–32.
36 P. R. Spackman, M. J. Turner, J. J. McKinnon, S. K. Wolff, D. J. Grimwood, D. Jayatilaka and M. A. Spackman, CrystalExplorer: A program for Hirshfeld surface analysis, visualization and quantitative analysis of molecular crystals, *J. Appl. Crystallogr.*, 2021, **54**, 1006–1011.

